www.sciencemag.org/content/355/6322/298/suppl/DC1

Supplementary Materials for

Mechanistic basis for a molecular triage reaction

Sichen Shao, Monica C. Rodrigo-Brenni, Maryann H. Kivlen, Ramanujan S. Hegde*

*Corresponding author. Email: rhegde@mrc-lmb.cam.ac.uk

Published 20 January 2017, *Science* **355**, 298 (2017)
DOI: 10.1126/science.aah6130

This PDF file includes:

Materials and Methods

Plasmids and antibodies

Model TA proteins in this study contained the Sec61β cytosolic domain and the TMD from either VAMP2 (Fig. 1 and 2) or Sec61β (Fig. 3 and 4). Expression in RRL and the PURE system used SP6- and T7-based plasmids as described (*6*, *24*, *31*, *32*). Constructs used for the expression and purification of recombinant proteins were as follows: His-tagged UBL4A and calmodulin (*32*) were in the pRSETA vector, His-tagged TRC40 was in the pET28 vector (*33*), GST-tagged TRC35 and SGTA were in the pGEX6P vector, FLAG-tagged BAG6 (*9*) was in the pcDNA FRT/TO vector, and GST-tagged TRC35 together with the cBAG6 fragment were in the pACYC-Duet1 vector. Mutated versions of recombinant proteins (C38S SGTA, G47Y UBL4A, R25D/K29D TRC35, E305R/D306R TRC40, L190D/I193D TRC40, ΔUBL BAG6, nBAG6) have been previously described (*9*, *10*, *24*), or were generated from the wild type versions by conventional techniques. Rabbit polyclonal antibodies raised against SGTA, UBL4A, BAG6, TRC40, and the N-terminus of Sec61β have been described (*6*, *9*, *16*).

In vitro transcription, RRL immunodepletions, and in vitro translation reactions

Templates for transcription were generated by PCR using a 5' primer that anneals just before the SP6 promoter in the SP64 vector and a 3' primer that anneals ~200 bp downstream of the stop codon of the open reading frame. Transcription reactions were carried out with SP6 polymerase for 1 hour at 37°C. Transcription reactions were directly used for in vitro translation in a homemade rabbit reticulocyte lysate (RRL)-based translation system as previously described (*34*). Unless otherwise indicated, translation reactions were at 32°C for 30 min. To assay for ubiquitination, 10 μM of His-tagged or FLAG-tagged ubiquitin (Boston Biochem) was included in the translation for downstream denaturing pulldowns. Factor(s) were immunodepleted from the RRL translation system by two sequential 20 min incubations at 4°C with Protein A beads conjugated to polyclonal antibodies raised against the factor(s). The immunodepleted RRL system was collected through gravity flow columns and used directly for translation or stored at -80°C for future use.

Recombinant protein purification

Recombinant RNF126 was purified as previously described (*10*). GST-tagged SGTA, His-tagged UBL4A, GST-tagged TRC35, His-tagged cBAG6, His-tagged TRC40, His-tagged BpF-RS (for amber suppression in the PURE system), His-tagged calmodulin, and the associated mutants were purified from *E. coli* (BL21) or (BL21)pLysS cells according to standard procedures. Briefly, cells were transformed with the expression plasmid encoding the protein and grown at 37°C in LB under the appropriate antibiotic selection. Induction was with 0.2 mM IPTG at an A_{600} of 0.4-0.6 at 37°C for 2 hours (GST-SGTA, His-UBL4A, His-TRC40, His-BpF-RS) or with 0.2 mM IPTG at an A_{600} of 0.7-0.8 at 16°C overnight (GST-TRC35 without or with cBAG6 co-expression). Cells were directly harvested, resuspended in ~12 mL cold lysis buffer [1X PBS, 250 NaCl, 1X protease inhibitor cocktail (Roche)] per L culture, and lysed by passing two times through a microfluidizer (Microfluidics, Inc.).

The lysates were clarified by centrifugation and bound to Ni-NTA or glutathione-sepharose columns by gravity flow. Columns were washed with ~10 column volumes of lysis buffer and elutions were carried out with 250 mM imidazole in lysis buffer (for His-tagged proteins) or with

10 mM glutathione in 25 mM Tris, pH 8.0 for GST-tagged proteins. Peak elutions as judged by A_{280} readings were pooled and dialyzed twice against dialysis buffer (50 mM Hepes, pH 7.4, 150 mM KOAc, 2 mM $MgAc_2$, 10% glycerol, 1 mM DTT). During the buffer change, 1:200 of SuperTEV (for His-tagged proteins) or 3C protease (for GST-tagged proteins) were added for overnight digestion, followed by subtraction of the proteases and cleaved tags by passage over the appropriate column by gravity flow.

To assemble the cBAG6 complex, GST-TRC35 coexpressed with His-tagged cBAG6 were first purified via a Ni-NTA column. The peak elutions were combined with ~5X molar excess of His-tagged UBL4A and dialyzed overnight in the presence of SuperTEV into 1X PBS, 10% glycerol, 1 mM DTT. The next day, the triple complex was purified via a glutathione-sepharose column, eluted as above, dialyzed into dialysis buffer in the presence of 3C protease, and subtracted by passing over a glutathione-sepharose column.

Full-length BAG6 and relevant mutants were transiently transfected into HEK293T cells with TransIT-293 (Mirus). Transfected cells were maintained for 3 days, harvested in ice cold PBS, and lysed in 50 mM Hepes, pH 7.4, 150 mM KOAc, 2.5 mM $MgAc_2$, 1% Triton X-100, 1X protease inhibitor cocktail (Roche), 1 mM DTT. The nuclei were removed by centrifugation, and the supernatant incubated with anti-FLAG (M2) agarose beads (Sigma) for 1 hour at 4°C. The column was washed with 3 mL of lysis buffer, 3 mL of lysis buffer with an additional 250 mM KOAc, and 3 mL elution buffer (50 mM Hepes, pH 7.4, 150 mM KOAc, 2.5 mM $MgAc_2$, 10% glycerol, 1 mM DTT). Two sequential elutions were carried out with 0.1 mg/ml 3XFLAG peptide (Sigma) in elution buffer for 25 min at room temperature. To generate full-length BAG6 complexes and subcomplexes, cell lysates expressing the appropriate BAG6 protein were incubated with ~10-fold excess of recombinant purified TRC35 and UBL4A (with tags cleaved off), and purified via the FLAG tag as above.

Chemical crosslinking and immunoprecipitations

Unless indicated otherwise, chemical crosslinking was with 250 μM DSS or BMH (Pierce) for 30 min at room temperature (DSS) or 1 hour on ice (BMH). Translations in RRL were diluted 10-fold in KHM buffer (50 mM Hepes, pH 7.4, 100 mM KOAc, 2 mM $Mg(OAc)_2$) before crosslinking. For direct analysis, crosslinking reactions were quenched with protein sample buffer and analyzed by SDS-PAGE. For immunoprecipitations, crosslinking reactions were quenched with 25 mM Tris (DSS) or 2.5 mM DTT (BMH) and denatured by the addition of 1% SDS and boiling. Denatured samples were diluted at least 10-fold in IP buffer (1X PBS, 250 mM NaCl, 1% Triton X-100) and incubated with the appropriate antibody and Protein A beads for 1-1.5 hours at 4°C. Beads were washed 2-3 times with 1 mL cold IP buffer and directly eluted in protein sample buffer.

Native affinity purifications

Native affinity purifications of endogenous SGTA (Fig. 1B) was performed with unmodified RRL or RRL immunodepleted of BAG6 and supplemented with native concentrations of the indicated factors. Ribosomes were removed from the lysates by centrifugation at 70K rpm in a TLA120.1 rotor (Beckman Coulter) for 30 min at 4°C. The supernatant was incubated for 20 min at 4°C with control Protein A beads conjugated to αGST polyclonal antibodies in a pre-clearing step. The beads were spun down and the pre-cleared supernatant was then incubated with control or Protein A beads conjugated to αSGTA antibody for 1 hr at 4°C. The beads were washed three times with 0.5X PSB (25 mM Hepes, pH 7.4, 50

mM KOAc, 1 mM $Mg(OAc)_2$, 1 mM DTT) + 0.5% TX-100, 3 times with 0.5X PSB, eluted with 1 mM SGTA peptide in 0.5 mM PSB for 20 min at room temperature, and directly analyzed by SDS-PAGE and immunoblotting.

TA protein affinity purifications (Fig. 1E) were performed with in vitro translations of FLAG-tagged TA protein in the RRL translation system immunodepleted and supplemented with the indicated factors. After translation, the reactions were centrifuged at 70K in a TLA120.1 rotor (Beckman Coulter) for 30 min at 4°C to remove ribosomes, and the supernatant incubated with FLAG (M2) agarose (Sigma) for 1 hr at 4°C. The beads were washed ten times with 1X PSB (50 mM Hepes pH 7.4, 100 mM KOAc, 2 mM $Mg(OAc)_2$, 1 mM DTT) and directly eluted with protein sample buffer for SDS-PAGE and immunoblotting or autoradiography.

PURE system translation reactions

Initial experiments used the PURE translation system from New England Biolabs as per the manufacturer's instructions. Experiments employing amber suppression used a homemade PURE translation system that was generated as originally described (*31*) except that it lacked RF1 and contained 25 A_{260} units of E. coli tRNA from a strain over-expressing $tRNA_{CUA}$, 50 µg/mL BpF-RS, and 0.1 mM BpF. Translation reactions in the homemade system were for 30 min at 37°C or 32°C. TMD-binding factors were added to translation reactions at 12 µM. 50 µl translation reactions were diluted to 200 µl with physiological salt buffer (PSB; 50 mM Hepes pH 7.4, 100 mM KOAc, 2 mM $MgAc_2$) and directly used for downstream assays or subjected to size fractionation on a 2 mL 5-25% sucrose gradient in PSB centrifuged for 5 hours at 4°C in a TLS-55 rotor with the slowest acceleration and deceleration settings. Eleven 200 µl fractions were collected, and the peak fractions containing the relevant TA complex were pooled (from the top, fractions 3-5 for SGTA-TA and TRC40-TA complexes, fractions 2-4 for CaM-TA complexes) for downstream reactions.

E. coli tRNA for the homemade PURE system was generated as described (*35*): a pEVOL-based plasmid expressing the suppressor $tRNA_{CUA}$ was transformed into *E. coli* BL21(STAR) cells and grown in 2xTY containing 22.4 mM glucose and 10 mg/L thiamine under antibiotic selection. Cells were harvested when they reached an A_{600} ~1.2-1.5, and lysed in 0.4 M KOAc pH 4 by passing two times through a microfluidizer (Microfluidics, Inc.). Lysates were clarified by centrifugation and extracted with an equal volume of phenol. The aqueous fraction was ethanol precipitated overnight. The precipitate was resuspended in 0.2 M KOAc pH 4, re-extracted with one volume of phenol, and extracted with one volume of chloroform. The aqueous fraction was ethanol precipitated overnight, the precipitate was resuspended in DEAE column buffer (20 mM Tris pH 7.4, 100 KCl, 1 mM DTT), passed over a DEAE column, and washed extensively with column buffer. Bulk tRNA was eluted with column buffer containing 250 mM NaCl, subjected to ethanol precipitation, and dissolved in H_2O to an A_{260} of ~650.

Ubiquitination, ER insertion, chaperone transfer, and photocrosslinking reactions

The TA-chaperone complex used in all reactions was at 650 nM with respect to the chaperone, and sub-stoichiometric levels of radiolabeled TA protein. This was added to reactions with equimolar amounts of the other triage factors, except RNF126 at 150 nM as indicated. Ubiquitination reactions also contained 75 nM E1, 250 nM E2 (UbcH5), 10 µM tagged ubiquitin (all from Boston Biochem), and an energy regenerating system (ERS: 1 mM ATP, 1 mM GTP, 12 mM creatine phosphate, and 20 µg/mL creatine kinase). Insertion reactions contained canine pancreas RMs at 5 A_{280} units final concentration. Ubiquitination reactions were at 32°C for 10

min, and other reactions were for the times indicated in individual figures. Insertion and ubiquitination reactions were analyzed directly by SDS-PAGE and autoradiography. For time-resolved photocrosslinking, aliquots were removed from transfer reactions at the indicated timepoints and immediately flash frozen in liquid nitrogen. Crosslinking was done on dry ice ~10 cm away from a UVP B-100 series lamp (UVP LLC) for 10 min. After crosslinking, reactions were thawed and directly added to protein sample buffer for SDS-PAGE and autoradiography analysis. Autoradiograms were quantified using ImageJ. Graphs, calculation of mean and SEM values, and fitting of kinetic equations were done in Excel or Graphpad Prism using standard procedures.

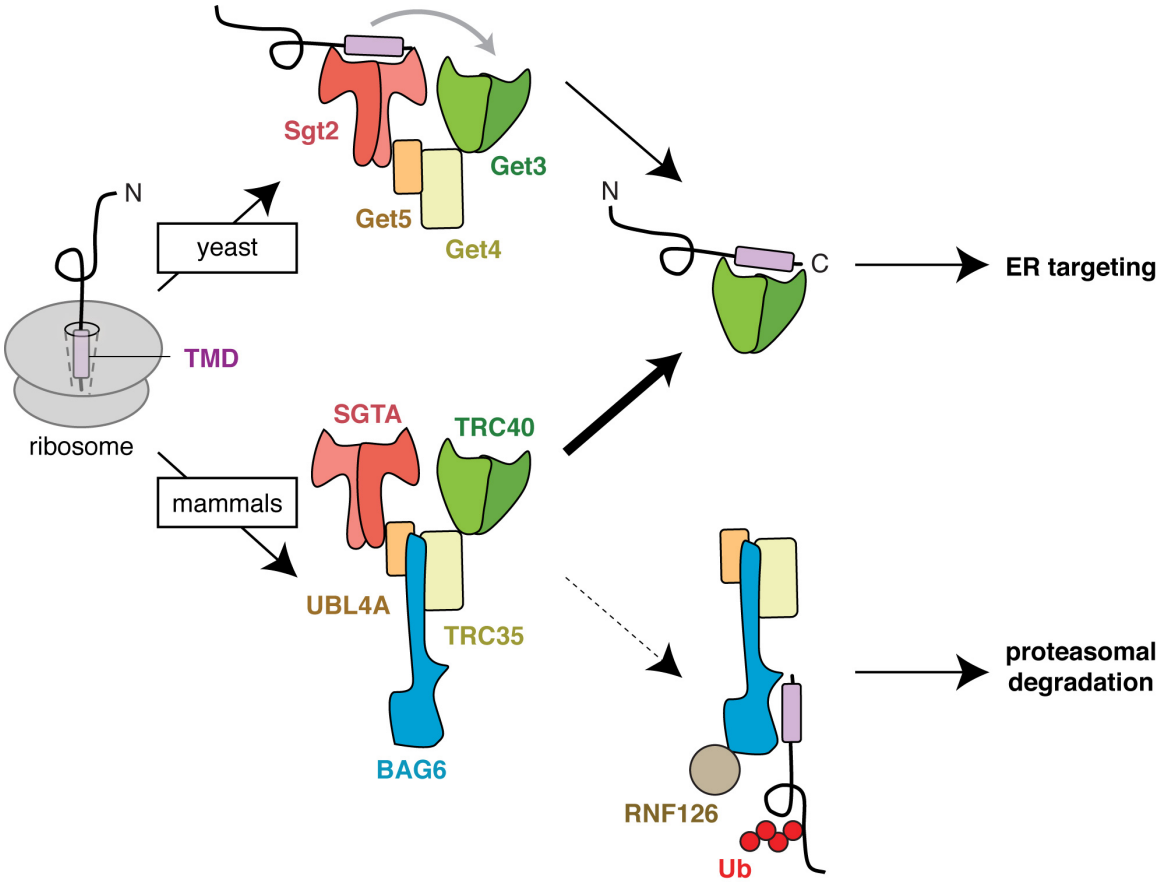

Fig. S1. TA protein biosynthesis in yeast and mammals.

Tail-anchored (TA) proteins, distinguished by having a single hydrophobic transmembrane domain (TMD) at the C-terminus, are posttranslationally inserted into the endoplasmic reticulum via a pathway conserved in eukaryotes. In yeast (top), this so-called Guided Entry of Tail-anchored (GET) pathway is centered around the targeting factor Get3, an ATPase that interacts with the Get1/2 ER membrane receptor complex to facilitate TA protein insertion (*7*, *12*, *13*, *36*). TA protein loading onto Get3 requires the heterodimeric Get4/5 pre-targeting complex (*11*, *24*, *37-40*), which physically bridges Get3 with Sgt2, another TA protein chaperone that captures ER-destined TA proteins released into the cytosol (*11*). TA protein targeting in mammals follows an analogous pathway centered around the Get3 homolog, TRC40 (*6*, *41*). Loading of TA proteins onto TRC40 requires the heterotrimeric BAG6 complex (*16*, *18*), which consists of TRC35 (homologous to Get4), UBL4A (homologous to Get5), and BAG6 (found widely across metazoans, but not in yeast). The BAG6 protein can also bind hydrophobic TMDs and interacts with the ubiquitin ligase RNF126 to mediate the proteasomal degradation of mislocalized membrane proteins in the cytosol (*9*, *10*, *20*, *42*). SGTA, the mammalian homolog of Sgt2, also interacts with the BAG6 complex and hydrophobic TMDs (*14*, *17*, *43*), and has been implicated by overexpression studies in modulating the degradation of mislocalized membrane proteins by an unclear mechanism (*17*, *19-21*, *43*, *44*). However, the function of SGTA in TA protein targeting or degradation remains poorly defined. Likewise, how the mammalian TRC system is able to triage TA proteins preferentially for targeting over degradation is not understood.

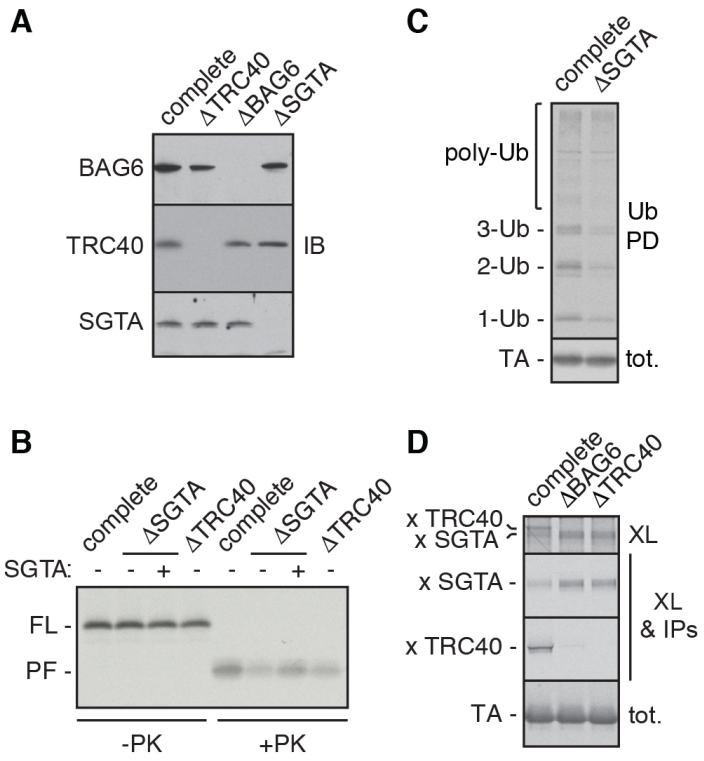

Fig. S2. Effect of triage component depletion on TA protein fate.

(A) Rabbit reticulocyte lysate (RRL) used for in vitro translation reactions was immunodepleted of the indicated components of the triage system and analyzed by immunoblotting. This shows that depleting one component does not affect the levels of the others. **(B)** ^{35}S-radiolabeled TA substrate containing the VAMP2 TMD was translated in complete RRL or RRL depleted of the indicated components. Where indicated, recombinant SGTA (SGTA) was added back at native levels. All reactions contained ER-derived rough microsomes to permit membrane targeting and insertion. The translation reactions were treated with proteinase K (PK) to reveal the amount of protected fragment (PF) representing substrate that had inserted into the ER membrane, where it is protected from protease digestion. FL refers to full-length substrate. Note that depleting SGTA impairs TA protein insertion, reflected in the decreased amount of PF. This level of impairment is comparable to that obtained when TRC40 is depleted, and can be rescued by adding back SGTA. **(C)** ^{35}S-radiolabeled TA substrate was translated in complete or SGTA-depleted RRL (ΔSGTA) in the presence of 10 μM of tagged ubiquitin. The translation reactions were directly analyzed by SDS-PAGE and autoradiography to verify equal translation (bottom), or subjected to denaturing pulldowns to enrich for ubiquitinated products (top), revealing that SGTA depletion impairs the level of substrate ubiquitination. **(D)** ^{35}S-radiolabeled TA substrate containing the VAMP2 TMD was translated in vitro in complete RRL or RRL immunodepleted of individual triage components as indicated. The translation reactions were subjected to chemical crosslinking (XL) with 250 μM DSS and analyzed directly, or after immunoprecipitations (IPs) with antibodies raised against the indicated factors. The non-crosslinked TA protein and the crosslinks to the indicated factors were visualized by autoradiography. This demonstrates that TA protein interaction with SGTA is enhanced by depleting BAG6 complex or TRC40 (lanes 2 and 3).

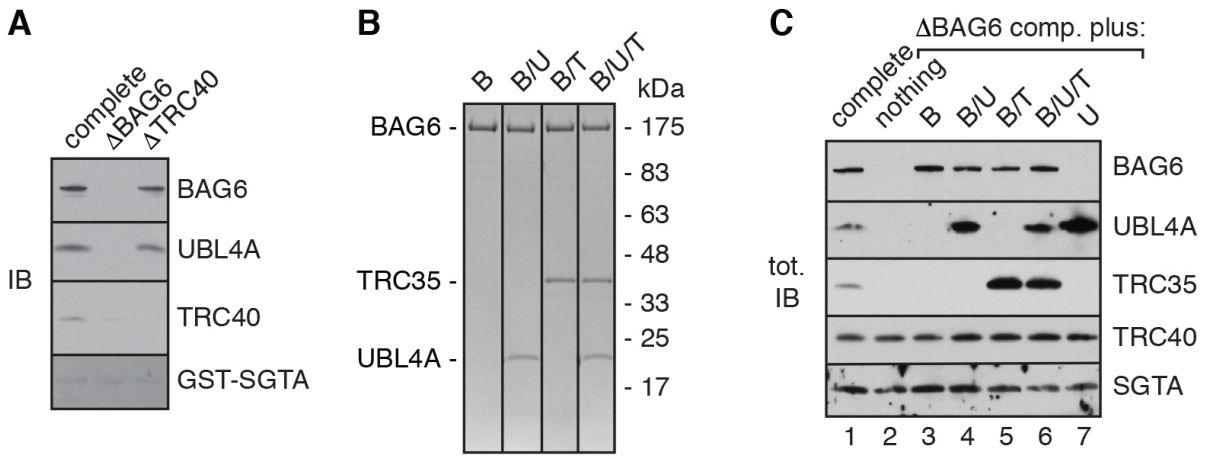

Fig. S3. Overall architecture of the triage system.

(A) RRL depleted of the indicated triage components was incubated with GST-SGTA and subjected to GST pulldowns under native conditions. The amount of GST-SGTA was visualized by Ponceau staining (bottom), while the co-precipitating partners were detected by immunoblotting (top). The result illustrates that the interaction between SGTA and TRC40 is dependent on the BAG6 complex. **(B)** Coomassie stain of purified recombinant BAG6 subcomplexes, with the BAG6 (B), UBL4A (U), and TRC35 (T) proteins labeled. **(C)** Immunoblots (IB) for triage components of control or BAG6 complex-depleted RRL replenished with recombinant BAG6 sub-complexes used for endogenous SGTA pulldowns and functional assays in Fig. 1B.

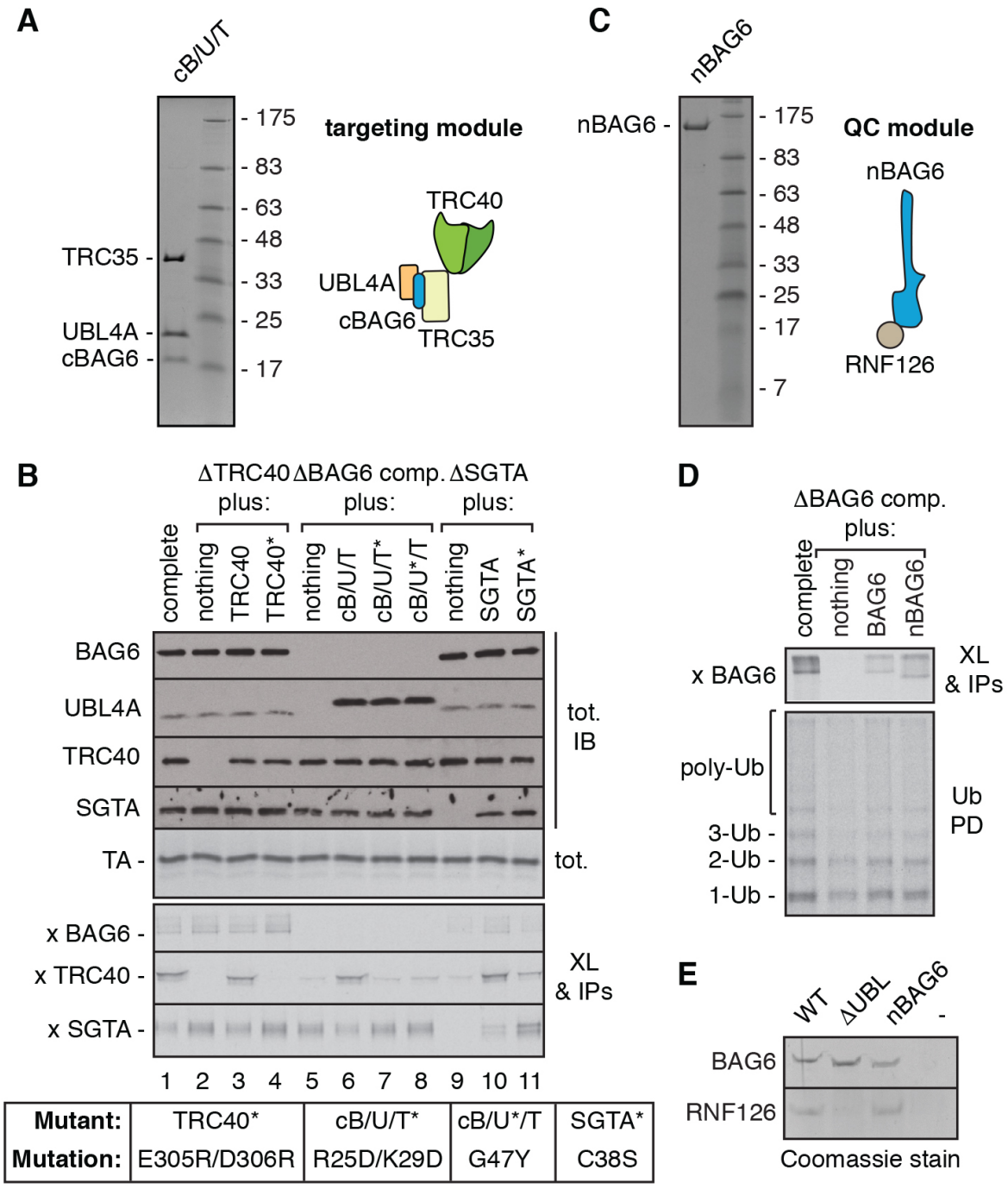

Fig. S4. The triage system is structurally and functionally modular.

(A) Coomassie stain (left) and schematic diagram (right) of the cBAG6 complex, comprising the C-terminal 100 amino acids of BAG6 (cBAG6/cB) in complex with UBL4A (U), and TRC35 (T). cB/U/T together with TRC40 (which interacts with TRC35) form the targeting module of the triage system that is sufficient to mediate substrate loading onto TRC40 for subsequent ER targeting. See also Fig. 1D. **(B)** ^{35}S-labeled TA protein (containing the VAMP2 TMD) was produced in either complete RRL or RRL depleted of the indicated components (indicated with

'Δ') replenished with nothing or recombinant wild type or mutant (*, exact mutations listed at bottom) versions of the depleted factors as indicated. The top panel shows immunoblots (IB) and autoradiography (to visualize ^{35}S-labeled TA protein) of the total translation reactions. These samples, which illustrate equal levels of TA protein translation and the composition and relative levels of each component of the triage system, were used for the pulldown experiment shown in Fig. 1E. In the bottom panel, these same samples were subjected to chemical crosslinking, immunoprecipitations for the indicated interacting partners, and analysis by SDS-PAGE and autoradiography to detect TA protein interactions. The pulldowns (without crosslinking; Fig. 1E) and the interactions detected by crosslinking show the same results: (i) the deficiency of TA protein capture by TRC40 upon depletion of BAG6 complex (lane 1 versus 5) can be fully restored by the cBAG6 complex (lane 6); (ii) TRC40 interaction with TRC35 (disrupted for TRC40* and TRC35*) is required for TA protein capture by TRC40 (lanes 4 and 7); (iii) SGTA interaction with UBL4A (disrupted by SGTA* and UBL4A*) is required for optimal TA transfer from SGTA to TRC40 (lanes 8 and 11); (iv) SGTA and its interaction with UBL4A are needed for optimal TA protein capture by BAG6 (lanes 9 and 11). **(C)** Coomassie stain of recombinant FLAG-tagged nBAG6 comprising the N-terminal 1007 amino acids of BAG6. The diagram shows that nBAG6, together with the E3 ubiquitin ligase RNF126, comprise the quality control (QC) module of the triage system that is ordinarily embedded in the targeting module shown in panel **(A)**. **(D)** TA protein translated in control or BAG6 complex-depleted RRL replenished with nothing or the individual recombinant BAG6 proteins as indicated. The translation reactions were subjected to chemical crosslinking followed by immunoprecipitations of BAG6 crosslinks (top), or ubiquitin pulldowns (bottom), demonstrating that nBAG6 can bind TA protein and restore the deficiency in ubiquitination activity seen with BAG6 complex depletion. **(E)** FLAG-tagged WT BAG6, ΔUBL BAG6, or nBAG6 was incubated with recombinant RNF126 and subjected to FLAG pulldowns, demonstrating a UBL-dependent interaction of RNF126 with the BAG6 protein (lane 1) that is also seen for nBAG6 (lane 3).

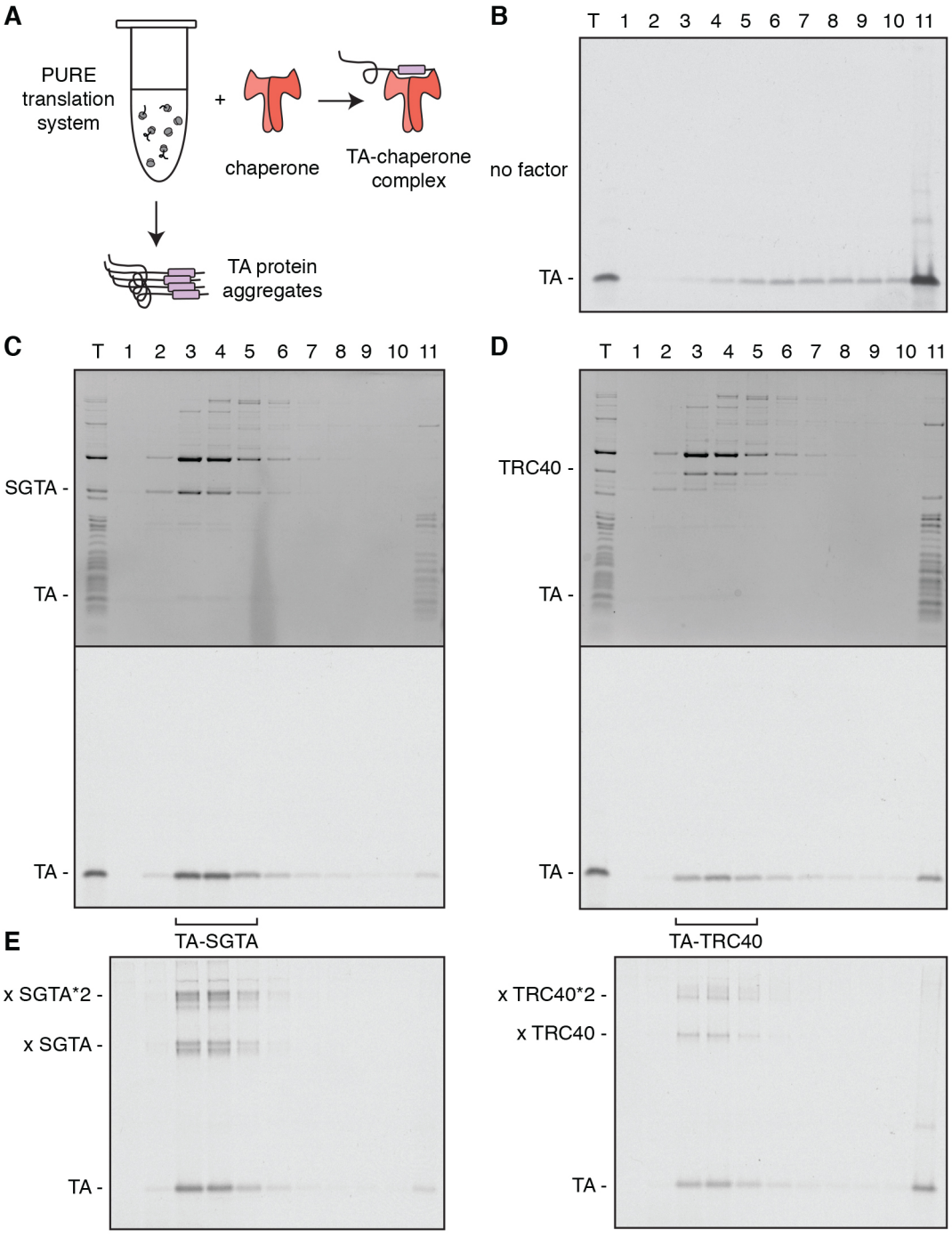

Fig. S5. TA-chaperone complexes produced using the PURE system.

(A) Schematic illustrating that translation of a TA protein in the chaperone-free reconstituted PURE translation system would lead to its aggregation, unless a TMD-binding chaperone is included during translation. **(B)** A model TA protein containing the VAMP2 TMD was translated in the PURE system in the presence of ^{35}S-methionine and size-separated into 11 fractions on a 5-25% sucrose gradient. The total reaction and each individual fraction were directly analyzed by SDS-PAGE and autoradiography. Fraction 1 is the top and fraction 11 is the bottom of the

gradient. Note that the TA protein migrates heterogeneously across the deeper parts of the gradient, with the majority in fraction 11, consistent with its aggregation. **(C)** A radiolabeled model TA protein containing the VAMP2 TMD was translated in the PURE system in the presence of 12 μM recombinant SGTA and size-separated into 11 fractions on a 5-25% sucrose gradient. The total reaction and individual fractions were analyzed by SDS-PAGE and Coomassie staining (top) or autoradiography (bottom). Note that the majority of the radioactive TA substrate migrates in fractions 3-5 together with SGTA, while ribosomes are observed in fraction 11. Fractions 3-5 (TA-SGTA protein complexes) were combined for downstream functional assays where such complexes were required. **(D)** As in panel **(C)**, but with 12 μM recombinant TRC40 included in the translation reaction instead of SGTA. **(E)** The individual fractions from the gradients in panels **(C)** and **(D)** were subjected to chemical crosslinking with 250 μM DSS and analyzed by SDS-PAGE and autoradiography, revealing homogenous substrate crosslinks to SGTA (left) and TRC40 (right) and their crosslinked dimers (*2), respectively.

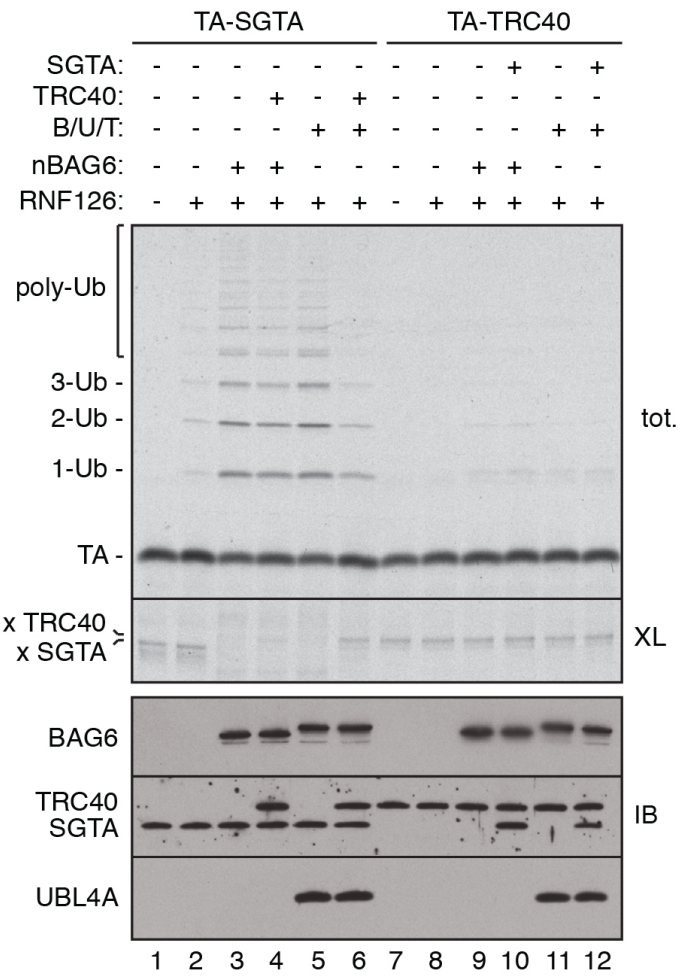

Fig. S6. Functionality of isolated TA-chaperone complexes.

Soluble TA-SGTA or TA-TRC40 protein complexes were isolated from PURE system translations (as in fig. S5; TA protein contains the VAMP2 TMD) and incubated with the indicated factors. Aliquots of the reactions were directly analyzed (tot.), subjected to chemical crosslinking (XL), or immunoblotted (IB) for the indicated factors. This revealed that TA protein preloaded onto SGTA was not effectively ubiquitinated by RNF126 (lane 2) unless nBAG6 (lane 3) or the complete BAG6 complex (B/U/T; lane 5) was also present. In these cases, the TA protein disengaged from SGTA as detected by crosslinking. When TRC40 is also included, it substantially reduces ubiquitination (lane 6) selectively in the presence of the complete BAG6 complex, concomitant with the appearance of TA-TRC40 crosslinks. By contrast, inclusion of TRC40 with nBAG6 has no effect on ubiquitination (lane 4), and capture by TRC40 is poor. Thus, TA protein is transferred from SGTA to BAG6 for ubiquitination in the absence of TRC40, but is preferentially transferred to TRC40 when the targeting module of the BAG6 complex is intact. By contrast to the situation with SGTA, TA protein preloaded onto TRC40 does not release from TRC40 (note the constant level of TA-TRC40 crosslinks in lanes 7-12) and does not support TA protein ubiquitination even in the presence of all of the other factors (e.g., lane 12). This suggests that over these time frames, TA protein on TRC40 is stable and does not transfer to the other TMD binding factors in the triage system.

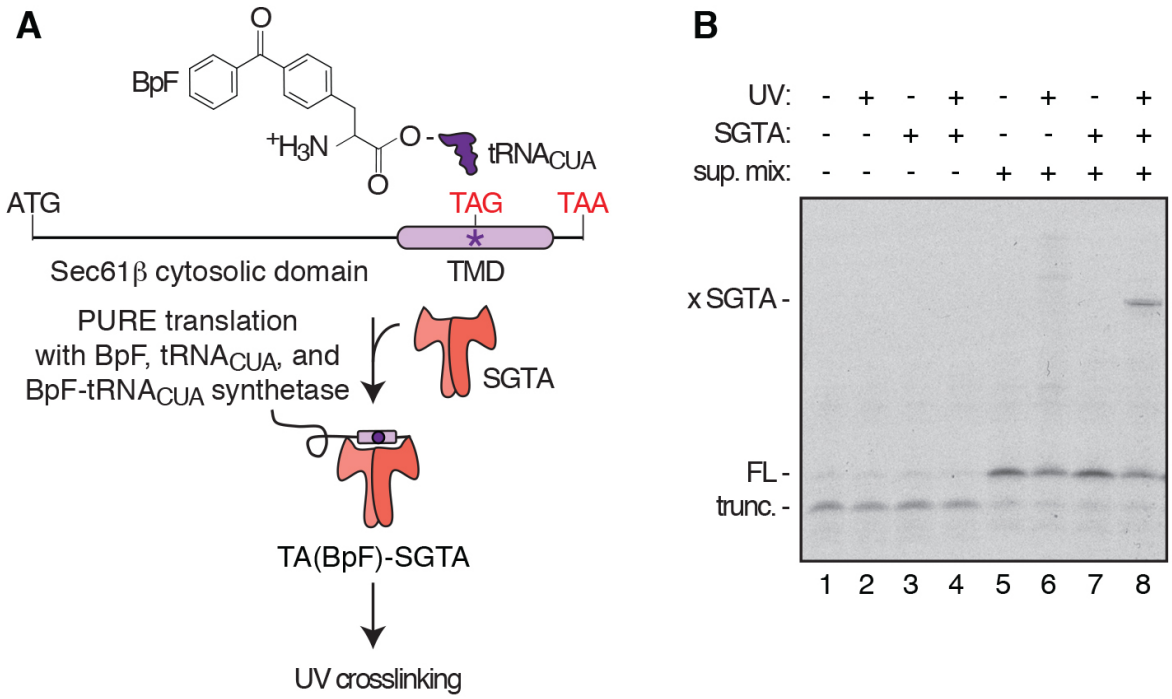

Fig. S7. Characterization of site-specific photocrosslinking.

(A) Schematic of the construct and strategy used to incorporate the non-natural UV-reactive amino acid p-benzoyl-p-phenylalanine (BpF) into the middle of the TMD of a model TA substrate to produce TA(BpF). This is achieved by amber codon (TAG) suppression in a homemade PURE translation system lacking RF1 (which normally recognizes amber codons), but containing the amber suppressor $tRNA_{CUA}$, the BpF-$tRNA_{CUA}$ synthetase, and BpF. Translation of such a construct in this modified PURE system supplemented with a TMD-binding chaperone, such as SGTA, produces TA(BpF)-chaperone complexes. This interaction can be directly probed via site-specific photocrosslinking by exposing the BpF-containing complex to UV light, a reaction that also works on frozen samples. **(B)** TA protein with an amber stop codon in the middle of the TMD was translated in the PURE system containing or lacking a suppression mix (sup. mix) containing BpF, $tRNA_{CUA}$, and BpF-$tRNA_{CUA}$ synthetase. Where indicated, SGTA was also included in the reaction. The suppression mix is required to effectively generate full-length (FL) protein (lanes 5-8) at the expense of truncated (trunc.) product terminated at the amber codon (lanes 1-4). UV irradiation on ice reveals a prominent crosslink to SGTA (lane 8), consistent with its direct interaction with the TMD.

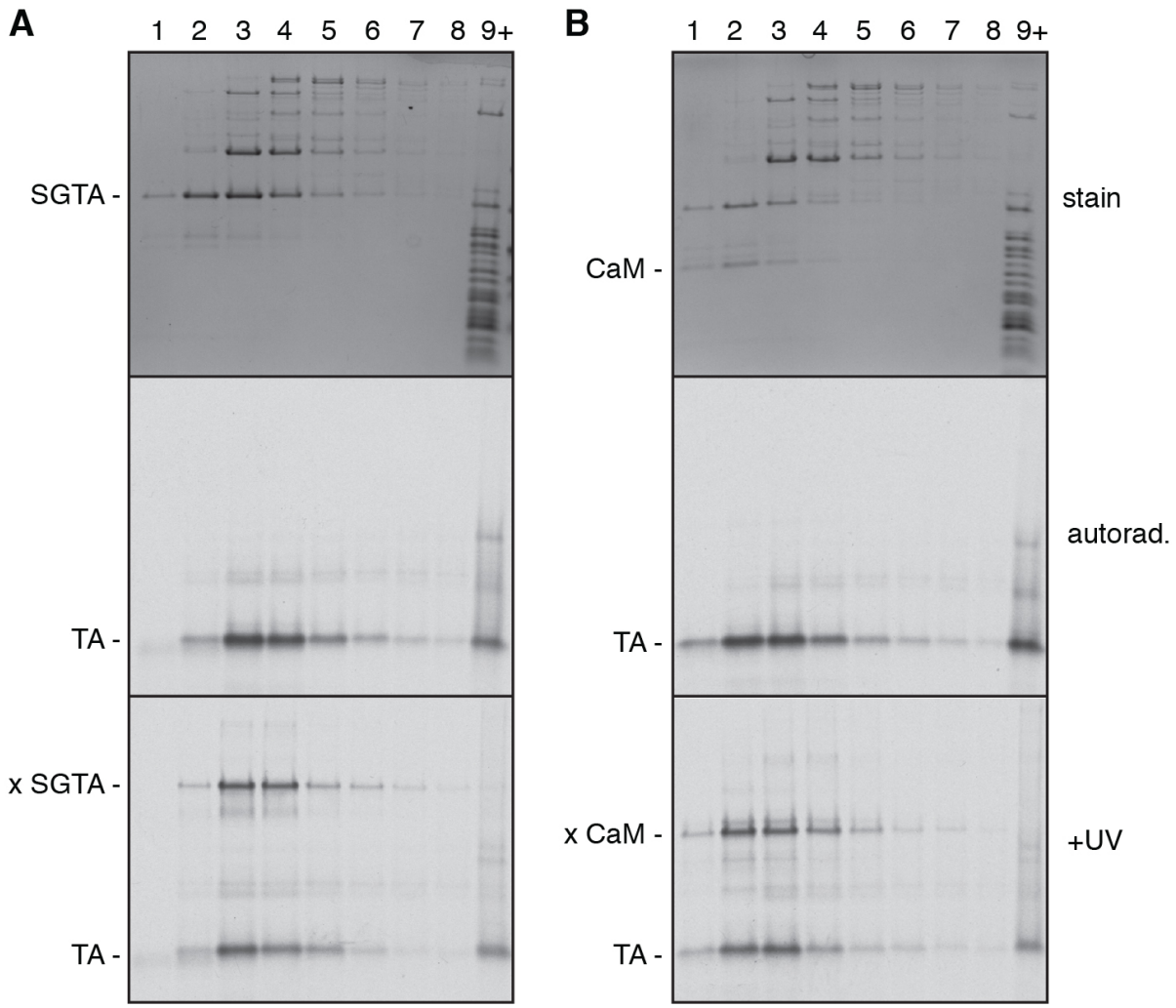

Fig. S8. Characterization of TA(BpF)-SGTA and TA(BpF)-CaM complexes.

(A) ^{35}S-labeled TA protein (WT Sec61β) containing an amber stop codon in the TMD was translated in a homemade PURE system incorporating BpF-amber suppression (see fig. S7) in the presence of 12 μM SGTA. The reaction was size separated on a 5-25% sucrose gradient, separated into 11 fractions (fraction 1 is the top of the gradient; fractions 9-11 were pooled), and analyzed by SDS-PAGE and Coomassie staining (top), or autoradiography (middle). The fractions were also exposed to UV light before SDS-PAGE and autoradiography, revealing photocrosslinks to SGTA indicative of direct interaction with the TMD of the TA protein. **(B)** Exactly as in panel **(A)** but with 12 μM CaM and 0.5 mM Ca^{2+}. The TA-CaM complexes migrate in fractions 2-4 of the 5-25% sucrose gradient, consistent with their smaller native size relative to TA-SGTA or TA-TRC40 complexes (see also fig. S5). Because CaM prefers to bind moderately hydrophobic amphipathic helices, the slightly less hydrophobic TMD of Sec61β (compared to VAMP2) facilitates CaM chaperoning the purified system, and was therefore used for all assays where TA protein was loaded onto CaM, or where excess CaM was used as a TA protein sink (see Fig. 3-4).

A

TRC Component	*S. cerevisiae*	*S. pombe*	*H. sapiens (HeLa)*	
SGTA (Sgt2)	32204	137012	277976	
UBL4A (Get5/Mdy2)	16977	35514	254088	
TRC35 (Get4)	6796	27365	64722	
TRC40 (Get3/ASNA1)	23128	138860	740041	
BAG6 (BAT3/Scythe)	N/A	N/A	79454	
RNF126	N/A	N/A	78735	
Ratios				**Average**
SGTA:TRC40	1.4	1.0	0.4	0.9
SGTA:TRC35	4.7	5.0	4.3	4.7
SGTA:BAG6	N/A	N/A	3.5	

B

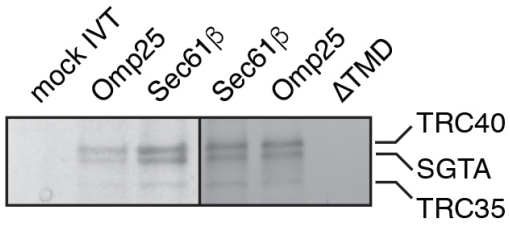

Fig. S9. Estimated physiologic concentrations of TRC chaperones
(A) Label-free quantitative mass spectrometry data from Kulak et al. (*45*) for the indicated proteins of the TRC system from three different organisms are shown. The top set of numbers show protein copy numbers, and the bottom the ratios between factors. We feel the most accurate comparisons are between SGTA, TRC40, and TRC35 because they are all similar in size and were represented by similar numbers of peptides with similar overall coverage in the dataset. By taking the average from these systems (assuming a high conservation of the pathway), we can estimate an approximate ratio of 1 SGTA: 1 TRC40: 0.2 BAG6 complex. Assuming that the volume of a Hela cell cytosol is 1 pL, the cytosolic concentration of TRC40 would be ~1.2 uM. Thus, we feel that assays performed at ~0.5 to 1 uM of factors will accurately represent the physiologic situation. **(B)** As an independent way of assessing abundance and stoichiometry, we directly visualized the levels of SGTA, TRC40, and TRC35 in reticulocyte lysate by Sypro staining after affinity purification of TA substrates that are translated at sufficiently high levels to saturate these chaperones. Independent experiments verified that at these levels of TA protein translation, they saturate all of these factors, and that the factors are depleted to comparable (~80-90%) levels from the lysate after affinity purification via the substrate. Several examples of such an experiment using different TA proteins from two independent trials shows a ratio of TRC40:SGTA:TRC35 that is consistent with the mass spectrometry analysis.

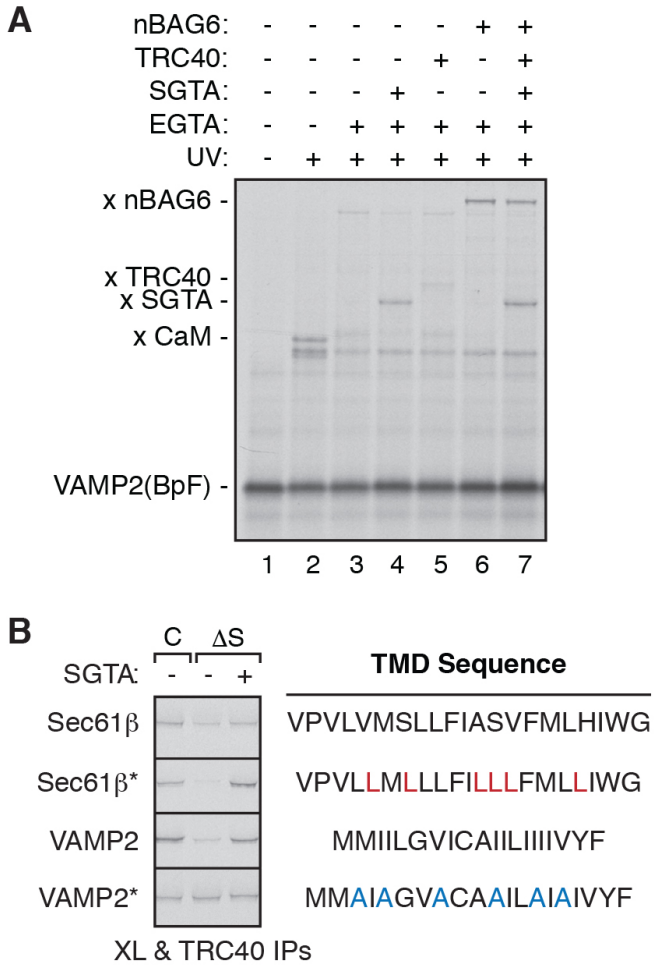

Fig. S10. Hydrophobicity of TA proteins influences dependence on SGTA.

(A) Radiolabeled TA protein containing the photocrosslinker BpF within the VAMP2 TMD [VAMP2(BpF)] was assembled with calcium calmodulin (CaM) using the PURE system (see fig. S8). Note that the translation reactions were carried out at 32°C instead of 37°C, as the slower translation rate at the lower temperature facilitates loading of the more hydrophobic TMD onto CaM. The VAMP2(BpF)-CaM complexes were then incubated with the indicated chaperones in the presence of 1 mM EGTA for 2 sec as in Fig. 3A, before being flash frozen and UV irradiated on dry ice. This shows that SGTA and nBAG6 both readily capture the TA protein after it is synchronously released from CaM (lanes 4 and 6, respectively). However, TRC40 captures VAMP2(BpF) less efficiently than a TA protein with a less hydrophobic TMD (lane 5, compare to Fig. 3B). **(B)** TA proteins containing TMDs with the indicated sequences were translated in control or SGTA-depleted (ΔS) RRL without or with recombinant SGTA added back. The reactions were subjected to chemical crosslinking and immunoprecipitated for TRC40 crosslinks to assay the efficiency of TA protein capture by TRC40. This shows that more hydrophobic TMDs are more dependent on SGTA for capture by TRC40. In the absence of SGTA, these hydrophobic TMDs are presumably more likely to make off-pathway interactions before their slow and inefficient capture by TRC40, whereas the less hydrophobic variants can be captured reasonably quickly by TRC40 (e.g., Fig. 3A).

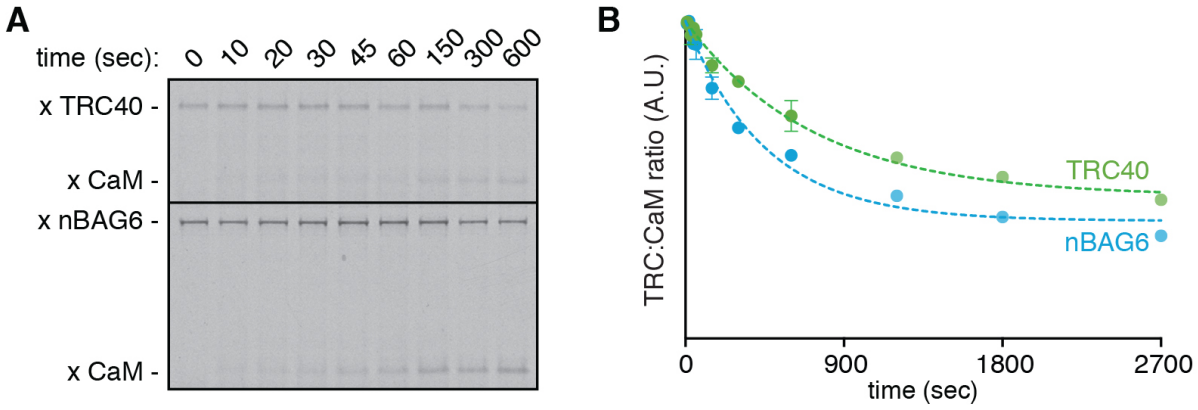

Fig. S11. TA protein release from TRC40 and BAG6.

(A) Time course of TA protein (WT Sec61β) release from TRC40 (top) and nBAG6 (bottom) monitored by site-specific photocrosslinking. TA(BpF)-CaM complexes (prepared as in fig. S8) were used to load the TA protein onto either TRC40 or nBAG6 (as in Fig. 3A). The resulting complexes were then added to a ten-fold molar excess of CaM and calcium. Aliquots were removed at the indicated timepoints, flash frozen in liquid nitrogen, and UV irradiated on dry ice to assay for TMD interactions. The autoradiograph of the reaction with TRC40 (top) and nBAG6 (bottom) are shown, and the TA protein crosslinks to TRC40, nBAG6, and CaM are indicated. **(B)** Quantification of TA(BpF) release from nBAG6 and TRC40 to an excess of CaM acting as a sink, as in **(A)**. Two timecourses for each condition were combined. Timepoints present in both timecourses (n=2) are opaque, representing mean values ± SEM; timepoints with only one value are transparent. Lack of error bars indicates an SEM that is smaller than the size of the datapoint. Dotted lines indicate a fitted single-exponential decay curve. Fig. 3E shows the same curves from 0-300 sec. Note also that the BAG6 complex displays indistinguishable kinetics of substrate release as nBAG6 using the same assay (data not shown). Although the kinetic parameters are not as reliable because the reactions do not reach completion, the fitted curves suggest that, compared to TA protein release from SGTA (Fig. 3, D and E), TA protein release is ~15-fold slower from BAG6, and ~30-fold slower from TRC40.

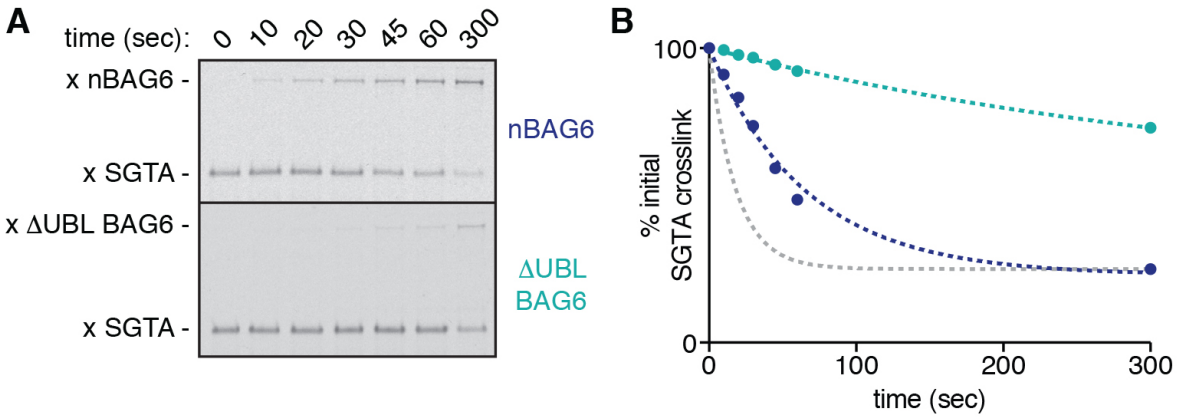

Fig. S12. Intact SGTA-BAG6 interactions facilitate TA protein transfer.

(A) Photocrosslinking timecourses measuring the transfer of TA(BpF) containing the Sec61β TMD from SGTA to nBAG6 (top) versus to ΔUBL-BAG6 (bottom). Transfer to nBAG6 is substantially faster than transfer to ΔUBL-BAG6, indicating that the interaction between SGTA and the UBL domain of BAG6 facilitates TA protein capture by BAG6. **(B)** Quantification of the reactions (n=1 each) from panel **(A)**, which were fitted with first order exponential decay equations and colored according to the labels next to each gel. The gray dotted line is the fitted equation for spontaneous TA protein release from SGTA (from Fig. 3E). This shows that substrate transfer from SGTA to nBAG6 is slower than the spontaneous TA protein dissociation rate from SGTA (gray line), while the transfer to ΔUBL-BAG6 is substantially slower still.

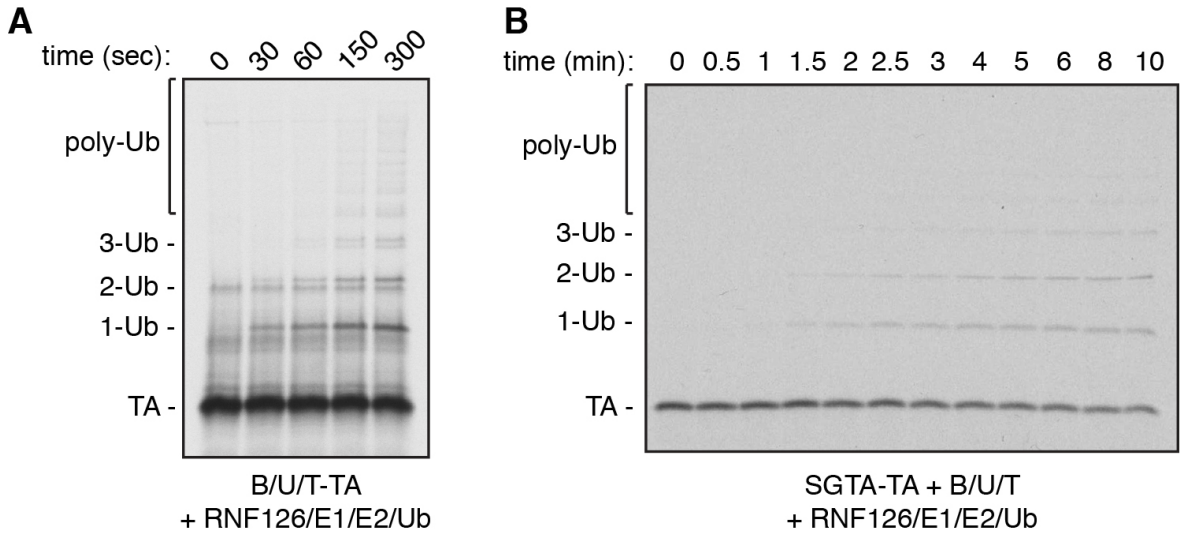

Fig. S13. TA protein ubiquitination.

(A) ^{35}S-methionine-labeled TA(BpF) containing the Sec61β was assembled onto the complete BAG6 complex (B/U/T) in the PURE translation system. The B/U/T-TA complexes were incubated with the ubiquitin ligase 150 nM RNF126, 75 nM E1, 250 nM UbcH5a, 10 μM His-tagged ubiquitin, and an energy regenerating system at 32°C. At the indicated timepoints, aliquots were removed from the reaction directly into SDS-containing protein sample buffer. The samples were analyzed by SDS-PAGE and autoradiography. B/U/T was present at 750 nM. Note that mono-ubiquitinated substrate can be observed after 30 seconds. **(B)** ^{35}S-methionine labeled TA protein containing the VAMP2 protein was assembled onto SGTA using the PURE translation system. SGTA-TA complexes were isolated by size fractionation on sucrose gradients. 750 nM of the resulting complexes (only a small proportion of which contains TA protein) was incubated with 750 nM B/U/T, 150 nM RNF126, 75 nM E1, 250 nM UbcH5a, 10 μM His-ubiquitin, and an energy regenerating system at 32°C and analyzed as in panel **(A)**.

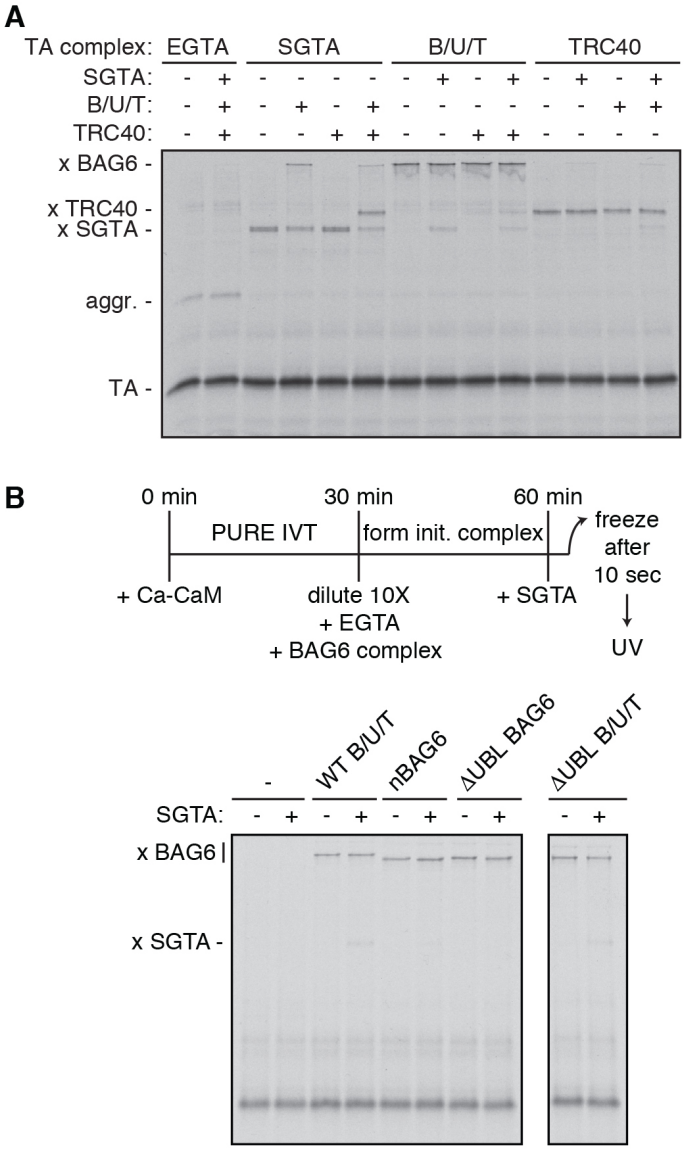

Fig. S14. TA protein transfer between TRC components.

(A) ^{35}S-methionine labeled TA(BpF) containing the Sec61β was translated in the PURE system in the presence of 0.5 mM calcium and 12 μM CaM. EGTA was used to form initial TA(BpF) complexes with the indicated TRC factor (complex) at 32°C for 30 min, which were then incubated with the other TRC components as indicated for 2 sec before being flash frozen and photocrosslinked to assess TMD interactions. **(B)** Experimental scheme (top) for assessing the ability of different BAG6 complexes to transfer a model TA(BpF) containing the Sec61β TMD to SGTA. TA(BpF)-CaM complex (see fig. S8) was used to load TA(BpF) onto the desired BAG6 complex as in Fig. 3A. The BAG6-TA(BpF) complexes were then incubated with SGTA for 10 seconds before being flash frozen and UV irradiated on dry ice. The reactions were analyzed by SDS-PAGE and autoradiography (bottom). Note that complexes containing UBL4A (in WT and ΔUBL B/U/T complexes), which can interact with SGTA, show detectable transfer of TA(BpF) from BAG6 to SGTA, while the absence of any UBL domain (ΔUBL BAG6) precludes TA(BpF) transfer to SGTA during the 10 sec incubation.

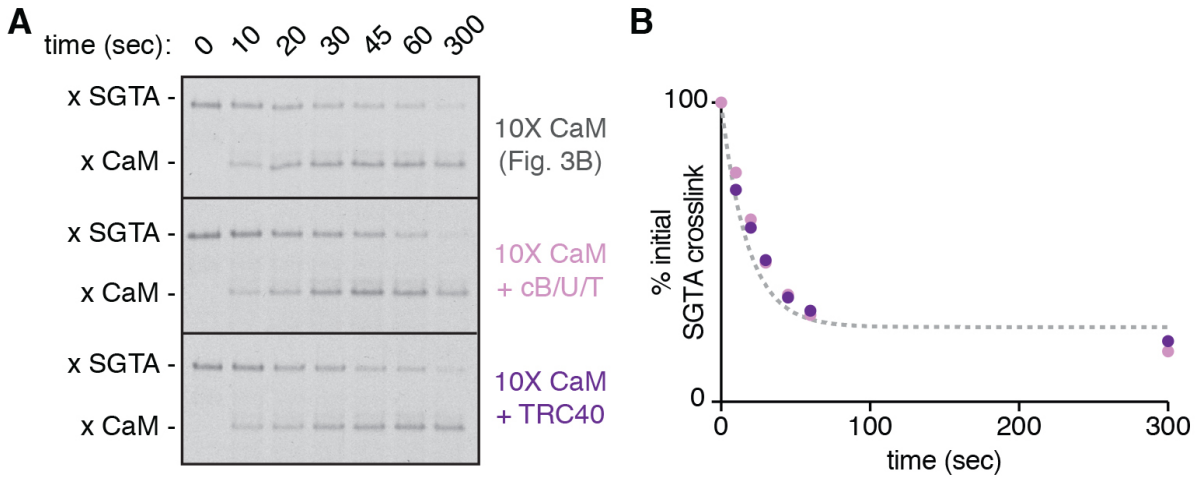

Fig. S15. cB/U/T and TRC40 do not independently induce release from SGTA.

(A) Photocrosslinking timecourses measuring the transfer of TA(BpF) containing the Sec61β TMD from SGTA to a ten-fold excess of CaM in the presence of the indicated components. The timecourse without any other components (top; reproduced from Fig. 3D) illustrates the rate of spontaneous TA(BpF) dissociation from SGTA. This baseline rate of release from SGTA is unchanged by the addition of the cBAG6 complex (cB/U/T), indicating that that SGTA interaction with this complex does not stimulate TA(BpF) dissociation. Likewise, TRC40 is ineffective at capturing TA(BpF) relative to CaM and does not induce faster release from SGTA, indicating that as an isolated TMD binding protein, it has no competitive advantage. **(B)** Quantification of the reactions in panel **(A)**, colored according to the labels next to the gel images. The gray dotted line is the fitted equation for the rate of spontaneous TA protein release from SGTA, as in Fig. 3E.

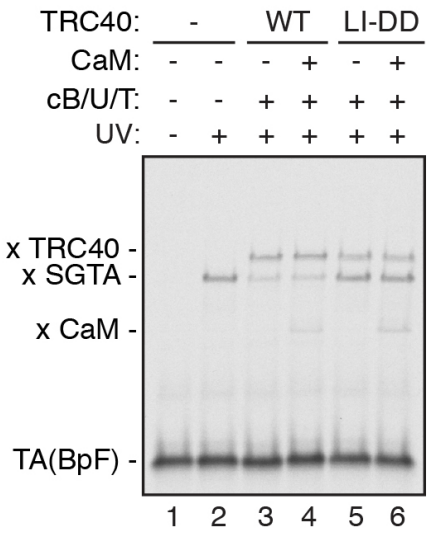

Fig. S16. An intact TRC40 binding site is required for private transfer.
On the basis of Get3 mutants described in Mateja et al. (*33*), TRC40 was mutated at two residues in the substrate binding groove (L190D/I193D; termed LI-DD) that are known to (partially) impair substrate binding without an appreciable effect on ATPase activity. This mutant was used in transfer assays from SGTA to TRC40 via the cBAG6 complex. 750 nM SGTA-TA(BpF) complexes (Sec61β) were incubated with equimolar amounts of cB/U/T and either wildtype (WT) or a substrate-binding mutant of TRC40 without or with 10X CaM at 32°C for 10 seconds before being flash frozen in liquid nitrogen and subjected to photocrosslinking by UV irradiation. Note that a greater amount of substrate is retained on SGTA in the reaction containing LI-DD TRC40 (lane 5) relative to the reaction containing WT TRC40 (lane 3), consistent with less transfer to mutant TRC40. This retention is not due to release and re-binding because inclusion of excess CaM in the reaction does not affect the amount of SGTA crosslinking to substrate (compare lanes 5 and 6). Thus, LI-DD TRC40, which has an intact TRC35 binding site but is partially impaired in substrate binding, does not induce TA protein release from SGTA beyond the population that is transferred to the mutant TRC40. Although a completely inert substrate binding mutant would have been ideal in this experiment, such a mutant is not available for two reasons. First, the substrate binding groove is very large, so single or even double mutants only moderately impair binding (*33*). Second, many of the mutants substantially affect other aspects of Get3/TRC40, such as destabilizing the open conformation and affecting its ATPase activity. Thus, it has not been possible to generate a mutant whose binding site is sufficiently altered to preclude substrate loading, while still maintaining other features of Get3/TRC40 structure and function. Nevertheless, the inability of a partial binding mutant to induce substrate release to the same level as WT TRC40 indicates that TRC40 engagement of the cBAG6 complex is not sufficient to trigger substrate release from SGTA.

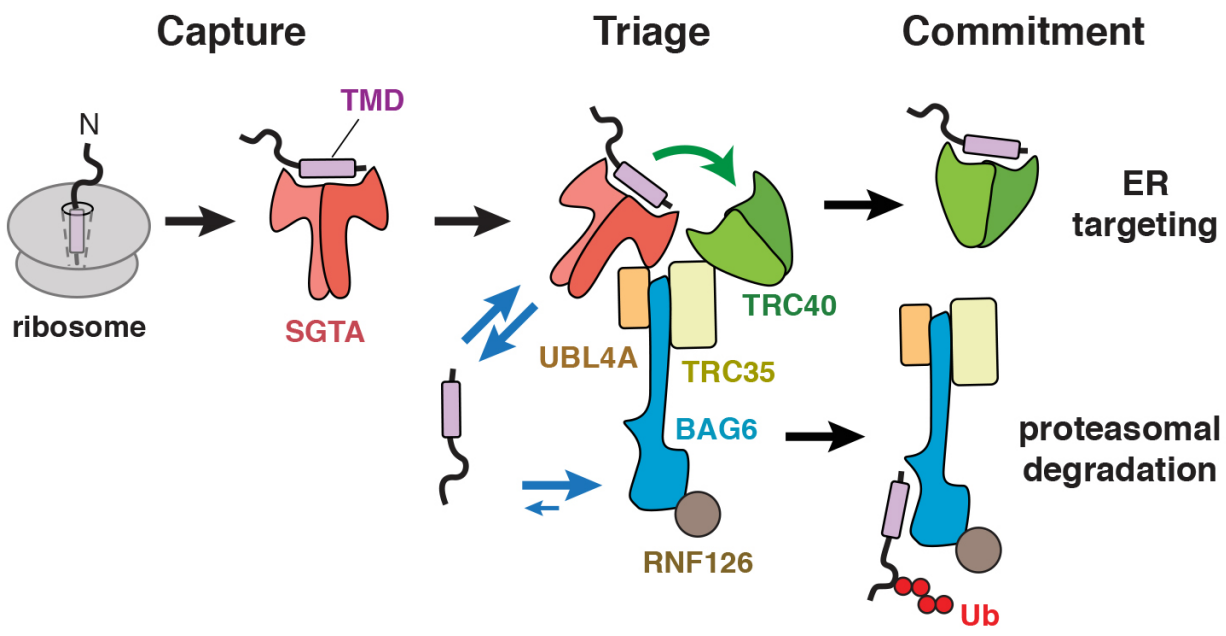

Fig. S17. Working model for TA protein triage.

Free nascent TA proteins are preferentially captured by SGTA (Fig. 3, A-C). The BAG6 complex bridges SGTA and TRC40 via the UBL4A and TRC35 subunits, respectively, in an architecture that allows for the rapid, concerted, and private handover of TA protein from SGTA to TRC40 (red arrow; see Fig. 4). The slow off-rate of TA proteins from TRC40 (Fig. 3, D and E) relative to the comparatively faster targeting to the ER membrane strongly favors TA protein targeting and biosynthesis. The small proportion of TA protein that spontaneously dissociates from SGTA before transfer to TRC40, or those that fail to load onto TRC40, are released in close proximity to the triage machinery. This free TA protein can be re-captured by either SGTA or BAG6, whose ability to capture these TA proteins is enhanced by a high local concentration (Fig. 3 and 4). TA protein has a slower off-rate from BAG6, providing opportunities to be ubiquitinated via the E3 ligase RNF126, which is relatively faster. Ubiquitination would bias substrates for proteasomal targeting. In this way, the quality control outcome is the default fate of the triage system. This mechanism imposes a time limit on how long nascent TA proteins are allowed to attempt biosynthesis, but results in a constitutive loss of productive maturation intermediates to degradation.

References and Notes

1. S. Shao, R. S. Hegde, Target selection during protein quality control. *Trends Biochem. Sci.* **41**, 124–137 (2016). doi:10.1016/j.tibs.2015.10.007 Medline

2. C. J. Guerriero, J. L. Brodsky, The delicate balance between secreted protein folding and endoplasmic reticulum-associated degradation in human physiology. *Physiol. Rev.* **92**, 537–576 (2012). doi:10.1152/physrev.00027.2011 Medline

3. C. Esser, S. Alberti, J. Höhfeld, Cooperation of molecular chaperones with the ubiquitin/proteasome system. *Biochim. Biophys. Acta* **1695**, 171–188 (2004). doi:10.1016/j.bbamcr.2004.09.020 Medline

4. S. Wolff, J. S. Weissman, A. Dillin, Differential scales of protein quality control. *Cell* **157**, 52–64 (2014). doi:10.1016/j.cell.2014.03.007 Medline

5. W. E. Balch, R. I. Morimoto, A. Dillin, J. W. Kelly, Adapting proteostasis for disease intervention. *Science* **319**, 916–919 (2008). doi:10.1126/science.1141448 Medline

6. S. Stefanovic, R. S. Hegde, Identification of a targeting factor for posttranslational membrane protein insertion into the ER. *Cell* **128**, 1147–1159 (2007). doi:10.1016/j.cell.2007.01.036 Medline

7. M. Schuldiner, J. Metz, V. Schmid, V. Denic, M. Rakwalska, H. D. Schmitt, B. Schwappach, J. S. Weissman, The GET complex mediates insertion of tail-anchored proteins into the ER membrane. *Cell* **134**, 634–645 (2008). doi:10.1016/j.cell.2008.06.025 Medline

8. R. S. Hegde, R. J. Keenan, Tail-anchored membrane protein insertion into the endoplasmic reticulum. *Nat. Rev. Mol. Cell Biol.* **12**, 787–798 (2011). doi:10.1038/nrm3226 Medline

9. T. Hessa, A. Sharma, M. Mariappan, H. D. Eshleman, E. Gutierrez, R. S. Hegde, Protein targeting and degradation are coupled for elimination of mislocalized proteins. *Nature* **475**, 394–397 (2011). doi:10.1038/nature10181 Medline

10. M. C. Rodrigo-Brenni, E. Gutierrez, R. S. Hegde, Cytosolic quality control of mislocalized proteins requires RNF126 recruitment to Bag6. *Mol. Cell* **55**, 227–237 (2014). doi:10.1016/j.molcel.2014.05.025 Medline

11. F. Wang, E. C. Brown, G. Mak, J. Zhuang, V. Denic, A chaperone cascade sorts proteins for posttranslational membrane insertion into the endoplasmic reticulum. *Mol. Cell* **40**, 159–171 (2010). doi:10.1016/j.molcel.2010.08.038 Medline

12. F. Wang, A. Whynot, M. Tung, V. Denic, The mechanism of tail-anchored protein insertion into the ER membrane. *Mol. Cell* **43**, 738–750 (2011). doi:10.1016/j.molcel.2011.07.020 Medline

13. M. Mariappan, A. Mateja, M. Dobosz, E. Bove, R. S. Hegde, R. J. Keenan, The mechanism of membrane-associated steps in tail-anchored protein insertion. *Nature* **477**, 61–66 (2011). doi:10.1038/nature10362 Medline

14. J.-Y. Mock, J. W. Chartron, M. Zaslaver, Y. Xu, Y. Ye, W. M. Clemons Jr., Bag6 complex contains a minimal tail-anchor-targeting module and a mock BAG domain. *Proc. Natl. Acad. Sci. U.S.A.* **112**, 106–111 (2015). doi:10.1073/pnas.1402745112 Medline

15. F. Vilardi, M. Stephan, A. Clancy, A. Janshoff, B. Schwappach, WRB and CAML are necessary and sufficient to mediate tail-anchored protein targeting to the ER membrane. *PLOS ONE* **9**, e85033 (2014). doi:10.1371/journal.pone.0085033 Medline

16. M. Mariappan, X. Li, S. Stefanovic, A. Sharma, A. Mateja, R. J. Keenan, R. S. Hegde, A ribosome-associating factor chaperones tail-anchored membrane proteins. *Nature* **466**, 1120–1124 (2010). doi:10.1038/nature09296 Medline

17. P. Leznicki, J. Warwicker, S. High, A biochemical analysis of the constraints of tail-anchored protein biogenesis. *Biochem. J.* **436**, 719–727 (2011). doi:10.1042/BJ20101737 Medline

18. P. Leznicki, A. Clancy, B. Schwappach, S. High, Bat3 promotes the membrane integration of tail-anchored proteins. *J. Cell Sci.* **123**, 2170–2178 (2010). doi:10.1242/jcs.066738 Medline

19. L. Wunderley, P. Leznicki, A. Payapilly, S. High, SGTA regulates the cytosolic quality control of hydrophobic substrates. *J. Cell Sci.* **127**, 4728–4739 (2014). doi:10.1242/jcs.155648 Medline

20. P. Leznicki, S. High, SGTA antagonizes BAG6-mediated protein triage. *Proc. Natl. Acad. Sci. U.S.A.* **109**, 19214–19219 (2012). doi:10.1073/pnas.1209997109 Medline

21. Y. Xu, M. Cai, Y. Yang, L. Huang, Y. Ye, SGTA recognizes a noncanonical ubiquitin-like domain in the Bag6-Ubl4A-Trc35 complex to promote endoplasmic reticulum-associated degradation. *Cell Rep.* **2**, 1633–1644 (2012). doi:10.1016/j.celrep.2012.11.010 Medline

22. J. W. Chartron, C. J. M. Suloway, M. Zaslaver, W. M. Clemons Jr., Structural characterization of the Get4/Get5 complex and its interaction with Get3. *Proc. Natl. Acad. Sci. U.S.A.* **107**, 12127–12132 (2010). doi:10.1073/pnas.1006036107 Medline

23. J. W. Chartron, D. G. VanderVelde, W. M. Clemons Jr., Structures of the Sgt2/SGTA dimerization domain with the Get5/UBL4A UBL domain reveal an interaction that forms a conserved dynamic interface. *Cell Rep.* **2**, 1620–1632 (2012). doi:10.1016/j.celrep.2012.10.010 Medline

24. A. Mateja, M. Paduch, H.-Y. Chang, A. Szydlowska, A. A. Kossiakoff, R. S. Hegde, R. J. Keenan, Structure of the Get3 targeting factor in complex with its membrane protein cargo. *Science* **347**, 1152–1155 (2015). doi:10.1126/science.1261671 Medline

25. S. M. Doyle, S. Wickner, Hsp104 and ClpB: Protein disaggregating machines. *Trends Biochem. Sci.* **34**, 40–48 (2009). doi:10.1016/j.tibs.2008.09.010 Medline

26. M. Coelho, I. M. Tolić, Asymmetric damage segregation at cell division via protein aggregate fusion and attachment to organelles. *BioEssays* **37**, 740–747 (2015). doi:10.1002/bies.201400224 Medline

27. V. A. Assimon, D. R. Southworth, J. E. Gestwicki, Specific binding of tetratricopeptide repeat proteins to heat shock protein 70 (Hsp70) and heat shock protein 90 (Hsp90) is regulated by affinity and phosphorylation. *Biochemistry* **54**, 7120–7131 (2015). doi:10.1021/acs.biochem.5b00801 Medline

28. J. C. Christianson, J. A. Olzmann, T. A. Shaler, M. E. Sowa, E. J. Bennett, C. M. Richter, R. E. Tyler, E. J. Greenblatt, J. W. Harper, R. R. Kopito, Defining human ERAD networks

through an integrative mapping strategy. *Nat. Cell Biol.* **14**, 93–105 (2012). doi:10.1038/ncb2383 Medline

29. L. A. Joachimiak, T. Walzthoeni, C. W. Liu, R. Aebersold, J. Frydman, The structural basis of substrate recognition by the eukaryotic chaperonin TRiC/CCT. *Cell* **159**, 1042–1055 (2014). doi:10.1016/j.cell.2014.10.042 Medline

30. A. Stein, A. Ruggiano, P. Carvalho, T. A. Rapoport, Key steps in ERAD of luminal ER proteins reconstituted with purified components. *Cell* **158**, 1375–1388 (2014). doi:10.1016/j.cell.2014.07.050 Medline

31. Y. Shimizu, T. Ueda, PURE technology. *Methods Mol. Biol.* **607**, 11–21 (2009). doi:10.1007/978-1-60327-331-2_2 Medline

32. S. Shao, R. S. Hegde, A calmodulin-dependent translocation pathway for small secretory proteins. *Cell* **147**, 1576–1588 (2011). doi:10.1016/j.cell.2011.11.048 Medline

33. A. Mateja, A. Szlachcic, M. E. Downing, M. Dobosz, M. Mariappan, R. S. Hegde, R. J. Keenan, The structural basis of tail-anchored membrane protein recognition by Get3. *Nature* **461**, 361–366 (2009). doi:10.1038/nature08319 Medline

34. A. Sharma, M. Mariappan, S. Appathurai, R. S. Hegde, In vitro dissection of protein translocation into the mammalian endoplasmic reticulum. *Methods Mol. Biol.* **619**, 339–363 (2010). doi:10.1007/978-1-60327-412-8_20 Medline

35. K. Ozawa, K. V. Loscha, K. V. Kuppan, C. T. Loh, N. E. Dixon, G. Otting, High-yield cell-free protein synthesis for site-specific incorporation of unnatural amino acids at two sites. *Biochem. Biophys. Res. Commun.* **418**, 652–656 (2012). doi:10.1016/j.bbrc.2012.01.069 Medline

36. S. Stefer, S. Reitz, F. Wang, K. Wild, Y.-Y. Pang, D. Schwarz, J. Bomke, C. Hein, F. Löhr, F. Bernhard, V. Denic, V. Dötsch, I. Sinning, Structural basis for tail-anchored membrane protein biogenesis by the Get3-receptor complex. *Science* **333**, 758–762 (2011). doi:10.1126/science.1207125 Medline

37. M. C. Jonikas, S. R. Collins, V. Denic, E. Oh, E. M. Quan, V. Schmid, J. Weibezahn, B. Schwappach, P. Walter, J. S. Weissman, M. Schuldiner, Comprehensive characterization of genes required for protein folding in the endoplasmic reticulum. *Science* **323**, 1693–1697 (2009). doi:10.1126/science.1167983 Medline

38. H. B. Gristick, M. E. Rome, J. W. Chartron, M. Rao, S. Hess, S. O. Shan, W. M. Clemons Jr., Mechanism of assembly of a substrate transfer complex during tail-anchored protein targeting. *J. Biol. Chem.* **290**, 30006–30017 (2015). doi:10.1074/jbc.M115.677328 Medline

39. M. E. Rome, M. Rao, W. M. Clemons, S.-O. Shan, Precise timing of ATPase activation drives targeting of tail-anchored proteins. *Proc. Natl. Acad. Sci. U.S.A.* **110**, 7666–7671 (2013). doi:10.1073/pnas.1222054110 Medline

40. H. B. Gristick, M. Rao, J. W. Chartron, M. E. Rome, S. O. Shan, W. M. Clemons Jr., Crystal structure of ATP-bound Get3-Get4-Get5 complex reveals regulation of Get3 by Get4. *Nat. Struct. Mol. Biol.* **21**, 437–442 (2014). doi:10.1038/nsmb.2813 Medline

41. V. Favaloro, F. Vilardi, R. Schlecht, M. P. Mayer, B. Dobberstein, Asna1/TRC40-mediated membrane insertion of tail-anchored proteins. *J. Cell Sci.* **123**, 1522–1530 (2010). doi:10.1242/jcs.055970 Medline

42. E. M. Krysztofinska, S. Martínez-Lumbreras, A. Thapaliya, N. J. Evans, S. High, R. L. Isaacson, Structural and functional insights into the E3 ligase, RNF126. *Sci. Rep.* **6**, 26433 (2016). doi:10.1038/srep26433 Medline

43. P. Leznicki, Q. P. Roebuck, L. Wunderley, A. Clancy, E. M. Krysztofinska, R. L. Isaacson, J. Warwicker, B. Schwappach, S. High, The association of BAG6 with SGTA and tail-anchored proteins. *PLOS ONE* **8**, e59590 (2013). doi:10.1371/journal.pone.0059590 Medline

44. P. Leznicki, J. Korac-Prlic, K. Kliza, K. Husnjak, Y. Nyathi, I. Dikic, S. High, Binding of SGTA to Rpn13 selectively modulates protein quality control. *J. Cell Sci.* **128**, 3187–3196 (2015). doi:10.1242/jcs.165209 Medline

45. N. A. Kulak, G. Pichler, I. Paron, N. Nagaraj, M. Mann, Minimal, encapsulated proteomic-sample processing applied to copy-number estimation in eukaryotic cells. *Nat. Methods* **11**, 319–324 (2014). doi:10.1038/nmeth.2834 Medline